An update and beyond: key landscapes for conservation land cover and change monitoring, thematic and validation datasets for the African, Caribbean and Pacific regions

Zoltan Szantoi[1,2], Andreas Brink[1], Andrea Lupi[1]

[1]European Commission, Joint Research Centre, 21027 Ispra, Italy
[2]Department of Geography and Environmental Studies, Stellenbosch University, Stellenbosch 7602, South Africa

Correspondence: Zoltan Szantoi (zoltan.szantoi@remote-sensing-biodiversity.org)

Abstract. Natural resources are increasingly threatened in the world. Threats to biodiversity and human well-being pose enormous challenges in many vulnerable areas. Effective monitoring and protection of sites with strategic conservation importance require timely monitoring, with a particular focus on certain land cover classes that are especially vulnerable. Larger ecological zones and wildlife corridors also warrant monitoring, as these areas are subject to an even higher degree of pressure and habitat loss as they are not 'protected' compared to Protected Areas (national parks, etc.). To address such a need, a satellite imagery-based monitoring workflow was developed to cover at-risk areas. The first phase of the programme covered a total area of 560 442 km^2 in sub-Saharan Africa. In this update, we remapped some of the areas using the latest satellite images available, and in addition we added some new areas to be mapped. Thus, in this version we have updated and mapped an additional 852 025 km^2 in the Caribbean, African and Pacific regions, involving up to 32 land cover classes. Medium to high spatial resolution satellite imagery was used to generate dense time series data, from which the thematic land cover maps were derived. Each map and change map was fully verified and validated by an independent team to meet our strict data quality requirements. The independent validation datasets for each key landscape for conservation (KLC) are also described and presented here (all datasets presented are available at https://doi.org/10.1594/PANGAEA.931968, Szantoi et al., 2021a).

1 Introduction

Key landscapes for conservation (MacKinnon et al., 2015) (KLCs) are defined as areas vast enough to sustain large wild animals (e.g. 'big five' game) within functioning biomes, that face pressure from various external factors such as poaching, agriculture expansion and urbanisation. Land use changes cause losses of both flora and fauna by altering wild animal movements, which can lead to decreases in population size over time (Di Minin et al., 2016; van der Meer, 2018). Livelihoods and wildlife in the Organisation of African, Caribbean and Pacific States (OACPS) that depend on natural resources face

increasing pressure due to consumption of resources by the growing population of the regions; for example, the population of Africa is set to reach 2 billion by 2040 (MacKinnon et al., 2015; Di Minin et al., 2016). The representative, often transboundary, location types of the KLCs uniquely position them as benchmarks for their natural resource management in generating steady income for local residents while protecting their wildlife (MacKinnon et al., 2015). Benchmarking activities of this kind require highly accurate thematic land cover change (LCC) map products. Although LCC maps exist for many areas within the regions, the majority of products only cover protected areas, with some buffer zones (Szantoi et al., 2016). Moreover, continental and global mapping efforts have reported thematic accuracies of such land cover maps as between 67% and 81%, with lower class accuracies reported in many cases (Mora et al., 2014). Differences in legends and unstandardised methods make these examples difficult to use for monitoring, modelling or change detection studies. In order to use various land cover (LC) and LCC products together (e.g. for modelling or policy-making), land cover class definitions should be standardised to avoid discrepancies in understanding thematic classes. Not all users (international organisations, national governments, civil societies, researchers) have the capabilities to readjust such maps (Saah et al., 2020). To accommodate such diverse user profiles, a common processing scheme is employed, and the resulting datasets can be utilised through various platforms and systems. This work adopted the Land Cover Classification System (LCCS) of the Food and Agriculture Organization of the United Nations (FAO) (Di Gregorio, 2005), an internationally approved ISO standard. The datasets presented in this paper are produced as part of the Copernicus High Resolution Hot Spot Monitoring (C-HSM) activity of the Copernicus Global Land Service.

All C-HSM products feature the same thematic land cover legend and geometric accuracy and were processed and validated following the same methodology. All products, including the C-HSM data, are free and open to any user with guaranteed long-term maintenance and availability under the Copernicus license.

Copernicus serves as an operational programme where data is produced on a continuous basis. This paper presents an update to four previously published (Szantoi et al., 2020b) land cover/change maps (Greater Virunga, Salonga, Upemba and Yangambi KLCs) covering 160 281 km^2 of terrestrial land area in sub-Saharan Africa (SSA), and six additional KLCs covering 691 744 km^2 in the OACPS regions. The datasets are based mainly on freely available medium spatial resolution data: Copernicus Sentinel-2 (S-2) data for maps after 2015, and United States Geological Survey Landsat 7 and 8 (LS7, LS8) data for maps before 2015. The exceptions are three areas (Caribbean, Timor Leste and Wapok) where we used *Centre national d'études spatiales* SPOT (SP4, SP5, SP6) data, because S-2 and LS7/8 had limited coverage for the time period we mapped. Each of the KLCs were individually validated for both present and change data. The processing chain developed always involves preliminary data assessment for availability, pre- and post-processing, and fully independent quality verification and validation steps. For the latter, a second dataset (validation data) is presented. Several recent studies call for sharing of product validation datasets (Fritz et al., 2017; Tsendbazar et al., 2018), especially if a collection received financial support through government grants (Szantoi et al., 2020a). Accordingly, the validation datasets (LC–LCC) associated with each of the KLCs are also shared.

2 Study area

The thematic datasets provided concentrate on sub-Saharan Africa, with additional KLCs in the Caribbean and Pacific regions. The areas were selected based on present and future pressures envisioned and predicted by MacKinnon and colleagues (2015) and the Biodiversity and Protected Areas Management (BIOPAMA) Programme (https://biopama.org). In this second phase (Phase 2), 10 large areas totalling 852 025 km^2 were selected, mapped and/or updated, and validated (Fig. 1). These areas cover various ecosystems and are generally located in transboundary regions (Table 1, Fig. 1). We selected four previously mapped KLCs (Szantoi et al., 2020b) to be remapped: Salonga (CAF07) because of the less detailed initial mapping (LCCS dichotomous level only), and Greater Virunga (CAF02), Upemba (CAF11) and Yangambi because of site importance identified by the BIOPAMA Programme and the Delegation of the European Union to DR Congo.

Figure 1 Spatial distribution of the key landscapes for conservation Phase 2 areas.

Table 1 Mapped key landscapes for conservation within Phase 2.

AB: Antigua and Barbuda; CAR: Central African Republic; DR: Dominican Republic; DRC: Democratic Republic of the Congo; SKN: Saint Kitts and Nevis.

3 Data and method

The production workflow for the entire process is shown in Figure 2. Each stage is explained in detail in the sections below.

Figure 2 Overall production workflow

3.1 Data collection and mapping guidelines

Landsat ETM+ and OLI at Level1TP, Sentinel-2 at Level1C, and SPOT 4, 5 and 6 at Level1-B imagery were used in producing and updating the land cover and change maps. As we previously developed a surface reflectance production chain in our workflow (Szantoi et al., 2020b), the Level1TP (Landsat), Level1C (Sentinel-2), and Level1-B (SPOT) data were further corrected for atmospheric conditions to produce such products for the classification phase. The atmospheric correction module was implemented based on the 6S direct radiative transfer model for Landsat (Masek et al., 2006) and SPOT (Haifeng et al., 2010), and using the Sen2Cor processor (v2.8) based on the ATCOR model (Richter et al., 2012). The Shuttle Radar Topography Mission (SRTM, 30 m or 90 m) digital elevation model was used to estimate the target height and slope, as well as the surface sun incidence angles to apply topographic correction. Based on the area's meteo-climatic conditions (climate profile and precipitation patterns), season-specific satellite image data were selected for each KLC (Table 1). Additionally, as

satellite data were limited for some of the mapped areas, especially for the years 2000 and 2005, imagery was collected for a target year (e.g. 2000) ± 3 years. In some cases, this was expanded to ± 5 years, or to where four cloud-free observations per pixel had been collected for the specified date and location.

3.2 Land cover classification system

All thematic maps were produced at both *Dichotomous* and *Modular* levels within the Land Cover Classification System (LCCS) developed by the FAO and the United Nations Environment Programme (Di Gregorio, 2005). The LCCS (ISO 19144-2) is a comprehensive hierarchical classification system that enables comparison of land cover classes regardless of geographic location or mapping date and scale (Di Gregorio, 2005). At the *Dichotomous* level, the system distinguishes eight major LC classes. At the *Modular* level, 32 LC classes were used (Table 2). For the Caribbean (CAR01), Timor-Leste (PAC01), and Madagascar (SAF21) KLCs, we included an additional land cover class not present in other KLC map products: 'Not Inland Cover'. Due to the specific location and the mapped areas (i.e. islands), this class is not present in LCCS and we only used it for our error assessment.

Table 2 Dichotomous and Modular thematic land cover/use classes (MCD: mapcode dichotomous level, MCM: mapcode modular level, AG: aggregated classes for land cover change accuracy estimation; see section 3.5 for additional information).

3.3 Image classification

Based on the imagery data (Appendix A), dense multitemporal timeseries (DMT) were generated to allow proper characterisation of the temporal variability of the spectral features through various vegetation indices, aiding the LC class labelling process. The DMT for each KLC was based on the pre-processed and geometrically co-registered data, forming a geospatial datacube (Strobl et al., 2017). Three vegetation indices were calculated to aid the separation of terrestrial vs aquatic (NDFI), vegetated vs barren (SAVI), and evergreen vs deciduous (NBR) vegetation areas.

The indices are (per Landsat spectral band):

Normalized Difference Flood Index (NDFI) $$NDFI = \frac{(RED - SWIR)}{(RED + SWIR)} \quad (1)$$

Soil-Adjusted Vegetation Index (SAVI) $$SAVI = \frac{1.5x(NIR - RED)}{(NIR + RED + 0.5)} \quad (2)$$

Normalized Burn Ratio (NBR) $$NBR = \frac{(NIR - SWIR)}{(NIR + SWIR)} \quad (3)$$

Imagery data (spectral bands and vegetation indices) were fed into the Support Vector Machine (SVM) supervised classification model. The SVM classifier can handle data with high dimensionality and performs well when mapping heterogeneous areas, including vegetation community types (Szantoi et al., 2013). To produce the thematic maps, the minimum

mapping unit concept used by Szantoi et al. (2016) was employed. Individual pixels (with corresponding land cover class information) were assigned to objects, where the minimum size of an object was set at 3 hectares (0.03 km^2), as a compromise between technical feasibility (pixel size) and the general size of the observable features (various land cover classes). However, classification errors (omission and commission of various classes) and false alarms (for land cover change) still occurred due to data availability (cloud cover, no data) and seasonal behaviour of the land cover (e.g. rapid foliage change). To correct these errors, expert human image interpretation skills and knowledge were applied, improving the outputs from the automated process.

3.4 Land cover change detection

Land cover change was interpreted as a categorical change in which one LC was replaced by another. Two examples of such a categorical change are the following: (1) conversion of cultivated and managed terrestrial areas (A11) into natural and semi-natural vegetation (A12); and (2) conversion of cultivated and managed terrestrial areas (A11) into artificial surfaces and associated areas (B15). LC change was identified based on detection of changes, employing the image-object overlay technique as a unit of analysis and hybrid change detection (Tewkesbury et al., 2015). This was achieved by applying layer arithmetic to locate changes such as (1) numerically compared spectral reflectance of the visible red and NIR bands and also derived indices such as NDFI, SAVI and NBR between the dates; and (2) classification to identify and label them (Lu et al., 2004).

LC changes were characterised as those lasting longer than a year and/or seasonal periodicity such as dry/wet seasons. Examples of longer-term changes include urban sprawl, large or small tree plantations replacing herbaceous crops, open or closed tree cover, or the creation of a reservoir. The LCC process applied followed the same steps for pre-processing earth observation images as the LC method. From the pre-processed time series imagery, selected indices such as SAVI were calculated and statistically aggregated over defined periods to generate temporal features such as the maximum SAVI for a defined monitoring period. Once the changes were located based on temporal feature arithmetic, the changes identified were labelled by the SVM classifier. For the classification, we collected training and validation datasets for the corresponding monitoring periods using visual interpretation.

Finally, visual interpretation using expert knowledge was used to correct classification errors, i.e. real vs mis-identified LC changes. When a within-object change was detected, the object was split. Similar to the creation of the LC product, visual interpretation and subsequent refinement were important steps in producing accurate LCC polygons.

3.5 Production of validation datasets

The validation datasets (Table 3, Figs. 3 and 4) were individually created for each KLC. The validation datasets (points) were generated using a stratified random sampling procedure. This ensured sufficient estimation of all land cover and land cover change classes according to their frequency of occurrence. The following formula (Gallaun et al., 2015) was used to determine the minimum number of validation points (per class per KLC):

$$n_c = \frac{p_c(1-p_c)}{\sigma_c^2}, c = 1, \ldots, L \quad (4)$$

n_c number of sampling units for class c

p_c estimated error rate for class c

σ_c accepted standard error of the error of commission for class c

L number of classes

In cases where classes covered smaller areas in total, additional sampling units were allocated according to Neyman optimal allocation, in order to minimise the variance of the estimator of the overall accuracy for the total sample size [n] (Gallaun et al., 2015; Stehman, 2012):

$$n_c = \frac{nN_c\sigma_c}{\sum_{k=1}^{L} N_k\sigma_k} \quad (5)$$

n_c sample size for class c

N_c population size for class c

σ_c estimated error rate for class c

L number of classes

N_k population size for class k

σ_k estimated error rate for class k

At least two independent data analysts evaluated all accuracy points (blind and plausibility interpretation process). Some points were excluded from the accuracy statistics due to an error/disagreement during the evaluation procedure (Table 3: 'Number of points LC/LCC'). The *blind* process attempted to interpret all validation points based on available ancillary data (i.e. higher resolution imagery), without direct comparison to the LC/LCC maps generated. The *plausibility* process reviewed every point where the blind interpretation did not match the corresponding LC/LCC value (disagreement between the LC/LCC data and the blind interpretation). After this review, the final validation reference was established.

Validation of the change maps (apart from CAF07, where we have assessed all the LCCS modular classes) aimed to assess the accuracy of the change detection. Thus, the following change categories were evaluated for those land cover changes (i.e. the accuracy assessments were done based on the aggregated LCCS classes below). The aggregated classes are also presented in Table 2.

- Loss of natural vegetation - change from vegetation classes to any other class
- Gain of natural vegetation - change from any class to vegetation classes
- Woody natural vegetation (forest) cover loss - tree cover to any other class

- Woody natural vegetation (forest) cover gain - change from any class to tree cover
- Woody natural vegetation (forest) degradation - change from closed forest to open forest
- Woody natural vegetation (forest) regeneration - change from open forest to closed forest
- Cultivated and managed (cropland) extension - change from any class to cultivated classes
- Artificial surfaces (human settlements) expansion - change from any class to built-up class

Table 3 Validation dataset attributes

Figure 3 Spatial distribution of the validation datasets within the updated key landscapes for conservation.

4 Data quality assessment

We updated some of the most critical landscapes (KLCs) due to various anthropogenic pressures for land cover change compared to the base maps we presented in Szantoi et al. (2020). These KLCs were Greater Virunga (CAF02), Salonga (CAF07), Upemba (CAF11) and Yangambi (CAF99). The Salonga KLC (CAF07) was initially mapped at the dichotomous LCCS level (Table 2, eight land cover classes), but here we present both the base map (2016) and a change map (2019) mapped at the modular LCCS level. The new land cover and land cover change maps (CAF05, CAR01, EAF04, PAC01, SAF21 and WAF04) were all mapped at the modular level for land cover as well as for change.

4.1 Technical Validation

Spatial, temporal and logical consistency was assessed using a procedure independent from the producer, to determine the products' positional accuracy, the validity of data with respect to time (seasonality), and the logical consistency of the data (topology, attribution and logical relationships). A qualitative accuracy assessment was also performed throughout, using a systematic visual examination for a) global thematic assessment, b) expected size of polygons (minimum mapping unit), c) seasonal effects, and d) spatial patterns (i.e. following correct edges).

Figure 4 Spatial distribution of the validation datasets within the new key landscapes for conservation.

The quantitative accuracy assessment (i.e. validation) results are shown in Table 4 (overall accuracies), and in the Appendix (thematic class accuracies per KLC, Appendix B). Generally, the programme aimed to achieve a minimum of 85% overall

accuracy for each product (KLC) and a minimum of 75% thematic accuracy (producer's and user's accuracy) for each class within each KLC. The land cover change accuracy should be > 72%. The requirements for C-HSM map accuracy were established based on users' needs, as accurate LC/LCC map products are needed for many applications – such as ecosystem modelling (Grafius et al., 2016) and ecosystem valuation (Foody, 2015) – besides the general need for accurate representation of ground cover for policy-making. The Copernicus Global Land Service defines the overall thematic accuracy of dynamic land cover mapping products as > 80% (Lang and Tychon, 2015). In exceptional cases, thematic accuracies may be lower than the threshold due to the difficulty of discriminating a particular class within a certain KLC.

Figure 5 shows the final LC and LCC products for the updated KLCs (CAF02, CAF07, CAF11 and CAF99), while Figure 6 (CAR01, WAF04), Figure 7 (CAF05, EAF04, SAF21) and Figure 8 (PAC01) show the new LC and LCC products, all classified at the modular LCCS level. Some of the datasets presented in Figure 5 had already been published in *Earth System Science Data* (Szantoi et al., 2020b): CAF02 year 2000 land cover change and year 2015 land cover maps; CAF07 year 2000 land cover change map; CAF11 year 2000 land cover change and year 2016 land cover maps; and CAF99 year 2000 land cover change and year 2016 land cover maps (for data access, please see the Data Availability section).

Table 4 Overall accuracies achieved for land cover mapping (%).

LC: land cover; LCC: land cover change.

Figure 5 Key Landscapes for Conservation - modular classification level. The boundaries (black polygons) represent protected areas (IUCN category I-IV – UNEP-WCMC and IUCN, 2021) within the KLCs. Both land cover and land cover change maps are presented for each KLC.

*CAF02: Greater Virunga; CAF07: Salonga; CAF11: Upemba; CAF99: Yangambi. Year 2000 datasets are available in Szantoi et al. (2020b).

Figure 6 Key landscapes for conservation - modular classification level. The boundaries (black polygons) represent protected areas (IUCN category I-IV – UNEP-WCMC and IUCN, 2021) within the KLCs. Both land cover and land cover change maps are presented for each KLC. The inlets show the south-east part of the Caribbean KLC.

*CAR01: Caribbean; WAF04: Wapok.

Figure 7 Key Landscapes for Conservation - modular classification level. The boundaries (black polygons) represent protected areas (IUCN category I-IV – UNEP-WCMC and IUCN, 2021) within the KLCs. Both land cover and land cover change maps are presented for each KLC.

*CAF05: Garamba; EAF04: Niassa Selous; SAF21: Madagascar.

Figure 8 Timor-Leste Key Landscape for Conservation - modular classification level. The boundaries (black polygons) represent the country boundary. Both land cover and land cover change maps are presented for Timor-Leste.

5 Discussion

There is a direct relationship between population growth, agricultural expansion, energy demand and pressure on land (Lambin and Meyfroidt, 2011). With the current state of development, population increase and economic growth, a large portion of the sub-Saharan population is dependent on the remaining natural resources to meet their food and energy needs (Brink et al., 2012), while in the Caribbean (CAR01), urbanisation is putting pressure on natural resources (Nathaniel et al., 2021). In the case of Timor-Leste (PAC01), the peacebuilding process has been shaping the country's land cover and land use trends since 2006 (Ide et al., 2021). The demands of social and economic growth call for additional land, typically at the expense of previously untouched areas. Areas under protection (i.e. national parks) that remain well-preserved (see Figs. 5, 6 and 7) are often in close proximity to regions under excessive pressure. In particular, transboundary areas – such as the mapped W-Arly-Pendjari Complex protected area (WAPOK) – highlight often strong spatial heterogeneity in anthropogenic pressure between the different countries (Bühne et al., 2017). Such areas need very accurate monitoring and base maps, as provided through this work, especially as areas shared between and/or among countries are frequently not mapped with a common legend, if mapped at all. The KLC datasets presented can be used for continuous land cover and land use monitoring, evaluation of management practices and effectiveness, endowment for scientific guidance, habitat modelling, information dissemination and capacity building in their corresponding countries, and to manage natural resources such as forests, soil, biodiversity, ecosystem services and agriculture (Tolessa et al., 2017). Furthermore, regional climate change, biogeochemical and hydrologic models are currently capable of using high-resolution LC data for general predictions (Nissan et al., 2019) and for spatially focused predictions (i.e. Africa) (Sylla et al., 2016; Vondou and Haensler, 2017).

The validation datasets are independently collected and verified through a robust procedure. The entire product validation procedure is systematically repeatable, as it includes three separate components that are independently assessed: (1) the spatial, temporal and logical consistency component, (2) the qualitative accuracy component, and (3) the quantitative accuracy component. Each of these components can be performed separately, with the use of standardised informatics tools. In particular, the quantitative assessment validation component is structured with a sequence of steps in which interpretation of the LC classes is iterated when a cover (or change) is in doubt. Furthermore, a random quality check of the interpretation is performed on 10% of the interpretation points. Validation datasets can then be used for additional land cover mapping, creating spectral libraries, and validating other local, regional and global datasets. It is important that various land cover products can be used or compared against one another regardless of their geographic origins. Here, 10 land cover and land cover change maps are introduced for various areas in the OACPS where quality land cover products were missing (Marshall et al., 2017).

All data were produced using the unified Land Cover Classification System. The modular level of the LCCS can be applied to local scales, thanks to its very detailed classes (32 were used here).

5.1 Drivers of change

Geist and Lambin (2002) describe the human forces driving land cover changes as an interlinking of three key variables: expansion of agriculture, extraction of wood, and development of infrastructure (urbanisation). The main land cover dynamic in sub-Saharan Africa can be explained by the first two variables, but increasingly also by urbanisation, as in the other areas mapped (Caribbean, Timor-Leste) (Güneralp et al., 2017; Nathaniel et al., 2021; Hugo, 2019). Although the driving force behind the clearing of natural vegetation has traditionally been predominantly attributed to the expansion of new agricultural land (including investments in large-scale commercial agriculture) (Brink and Eva, 2009), firewood extraction and charcoal production are also key factors in forest, woodland and shrubland degradation throughout the region. This land cover dynamic is not just a by-product of greater forces, such as logging for timber and agricultural expansion, but stems from a specific need to satisfy energy demand (European Commission, 2018); in fact, in sub-Saharan Africa, the main use of extracted wood is for energy production (Kebede et al., 2010). Although the region possesses a huge diversity of energy sources such as oil, gas, coal, uranium and hydropower, the local infrastructure and use of these commercial energy sources are still somewhat limited. Traditional sources of energy, in the form of firewood and charcoal, account for over 75 % of total energy use in the region (Kebede et al., 2010). Efforts to meet population and economic demands in the OACPS, while preserving biodiversity and ecosystem functioning, require informed decision-making. The global component of the Copernicus Land Monitoring Service (Copernicus Global Land Service), in particular the High Resolution Hot Spot Monitoring activity, presents a unique opportunity for such information gathering.

5.2 Sources of errors

As the LCCS applied allows very detailed hierarchical classification, some classes can be difficult to distinguish from each other. This is especially true in Africa's vast and highly heterogeneous landscapes, where agricultural land use is mainly smallholder-based (i.e. very small plots), while shifting cultivation is mostly due to the lack of fertilisers and weak soil, leading to land abandonment. Landscapes are generally not composed of clearly fragmented and well-identifiable cover formation. In this region, landscapes usually form a continuum of various cover (vegetation) formations, which may include different layers of tree, shrub and herbaceous vegetation. These variations, combined with differences in vegetation density (open vs closed) and heights, makes it challenging to assign classes. Moreover, some specific agricultural classes even distinguish the cultivation type, e.g. differentiating between fruit tree plantations and timber plantations. Thus, it is very difficult to discriminate between such classes, and classification errors may be introduced. Apart from the land cover classification, errors could also be introduced due to climate-induced variability – such as leaf phenology, where deciduous vegetation may appear bare during a dry period (season). At a more general level, difficulties in distinguishing between aquatic or regularly flooded surfaces and terrestrial areas have been observed in certain KLCs, especially when flooded periods are short. The difficulty in

interpreting some LC classes, as presented in the examples above, *might* introduce systematic over- and/or under-estimation of these particular covers in the accuracy statistics. The bias is reduced, for example, by giving higher weight to the errors in less represented LC classes depending on the ratio of ground control points collected per class, while the uncertainty of the LC class interpretation is quantified by calculating the confidence intervals (per class) in the statistics.

In the case of Timor-Leste (PAC01), it was particularly challenging to discriminate between evergreen and deciduous natural vegetation across the seasonal variations.

Another specific source of error can be identified for the Caribbean KLC (CAR01), where the area consists of a vast complex of small islands (i.e. keys) and archipelagos that include large areas of coastal swamps. In these regions, the connection of the coastal inland water surfaces with the open sea is often very difficult to identify. Consequently, there are areas where assignment of the water surface classes was ambiguous with respect to the open sea, which would result in the exclusion of areas from the map.

5.3 Current and future use of datasets

The C-HSM datasets have been widely used by policy-makers (OACPS and European partners) to help identify areas prone to change due to human activities. For example, COFED (Support Unit for the National Authorising Officer of the European Development Fund) DRC – the EEAS (European External Action Service) in the DRC – manages an envelope of EUR 120 million allocated for five protected areas in the DRC (Virunga, Garamba, Salonga, Upemba and the Yangambi biosphere), where they use the C-HSM products for planning and for investment strategies (e.g. hydropower). Thus, the EEAS requested updates in terms of land cover changes for 2019 for the above-mentioned protected areas, which we present in this study. Another example is from West Africa, where non-governmental organisations (NGOs, e.g. the Wild Chimpanzee Foundation), public benefit enterprises (e.g. German Society for International Cooperation – GIZ), and national authorities (e.g. *Office Ivoirien des Parcs et Réserves* – OIPR) use the data to identify areas under pressure for agriculture (cocoa, oil palm, rubber and coconut) and human–wildlife conflicts in Cote d'Ivoire, Ghana and Liberia. Additional areas (CAR01, PAC01) mapped and presented in this study can be used to help projects (e.g. BIOPAMA) and countries to improve management and governance of their biodiversity and natural resources.

6 Data availability

The data are provided in a shapefile (*.shp) format, polygon geometry for the land cover and change datasets, and point geometry for the validation datasets. The data presented are in the World Geodetic System 1984 geographic coordinate system (GCS) (EPSG:4326) and its datum (EPSG:6326). The validation data, besides using the same GCS, also use the Africa Albers Equal Area Conic (EPSG:102022) projected coordinate system.

Apart from CAF05 and PAC01, each KLC is described by two polygon vector layers: a land cover (LC) layer and a land cover change (LCC) layer. In the case of CAF05, we present three layers (2000 and 2019 as LCC, and 2017 as LC), and for PAC01 we present four layers (2000, 2005 and 2010 as LCC, and 2016 as LC). The LC layer is always a wall-to-wall map, covering the entire area of interest (AOI). The LC temporal reference for the project is the year 2016, although for each area the actual 'mapping year' is noted in the file name (e.g. CAF05_2017); this generally refers to the year from which the largest number of satellite images were used for the classification. The LCC layer provides partial coverage of the AOI, as it contains only the areas (polygons) where thematic change occurred compared to the LC layer. The LCC temporal reference is the year 2000 (± 3 years), noted in the file name (e.g. CAF05_2000).

Each LC and LCC shapefile comes with its corresponding attribute table, where two or three attributes are present: [map_codeA] – dichotomous class, [map_code] – modular class, [class_name] – corresponding modular class name.

Each of the 10 areas has been quantitatively validated using a spatially specific point dataset. These datasets were generated through the method described in section 3.5, and each point was used to verify the correctness of the LC–LCC maps. The corresponding data in the attribute table are LC – [plaus201X] and LCC – [plaus200X or plaus201X]. Both [plaus201X] and [plaus200X] attributes refer to the most detailed classification level attributes (map_code or map_codeA) present in the LC and LCC datasets (shapefiles). Some of the validation datasets contain only attributes of the aggregated classes, as described in section 3.2; those attributes are named as [plaus201Xr, plaus200Xr]. The plaus201X and plaus200X attributes refer to the year the validation sets represent, as these can be different among KLCs; the exact year is always noted in the column names (e.g. plaus2000, plaus2016).

The naming of all attributes follows the same structure for all data. Please see the details in Appendix B.

The datasets are available for download, as a complete package (all datasets together) or individually as source datasets (each KLC), from https://doi.org/10.1594/PANGAEA.931968 (Szantoi et al., 2021a) and https://doi.org/10.5281/zenodo.4621375 (Szantoi et al., 2021b).

Besides archiving the datasets at Zenodo (www.zenodo.org) (last access: 1 June 2021) and PANGAEA (www.pangaea.de) (last access: 1 June 2021) with corresponding digital object identifiers, the Copernicus High Resolution Hot Spot Monitoring (C-HSM) website (https://land.copernicus.eu/global/hsm, last access: 1 June 2021) provides open access to all the land cover and land cover change maps presented in this article, as well as technical reports and on-the-fly statistics.

7 Conclusions

The C-HSM component is part of the Copernicus Global Land Service, which produces near real-time biophysical variables at medium scale, globally. By contrast, the C-HSM activity is an on-demand component that addresses specific user requests

in the field of sustainable management of natural resources. The products presented here provide the second set of standardised land cover and land cover change datasets for 10 KLCs in the African, Caribbean and Pacific regions, with their corresponding validation datasets. The geographic distribution covers the tropical and subtropical regions of west, central and south-eastern Africa, as well as a large part of the Caribbean region and Timor-Leste in the Pacific region. The most recent land cover change may be periodically reassessed for selected already mapped KLCs, in order to generate longer-term time series land cover dynamics information, as is the case for some of the data presented here (CAF02, CAF07, CAF11 and CAF99 – see the original LC/LCC data in Szantoi et al., 2020b). Although this is done not systematically but at specific customer request, the C-HSM service encourages stakeholder cooperation and provides capacity building workshops around the globe. In-person training events provide an opportunity for new and existing users to learn how to use and interpret data, operate the web information system, and easily assess recent land cover change data using Sentinel-2 image mosaics. Here, we provide very high quality products, which can be used directly as base maps and for policy decisions, as well as for comparison and/or evaluation of other land cover products, or the implementation of validation datasets for training and validation purposes.

Finally, the service has a high degree of confidence that the data presented here (and in the previous phase, Szantoi et al., 2020b) are of the highest quality, regularly reaching above 90% overall accuracy. This is guaranteed by a rigorous and independent production and validation mechanism and feedback loop, which does not stop until the required overall and per-class accuracy levels are reached.

In accordance with the general European Commission open access policy for the Copernicus Programme, the data are distributed free to any user, through a dedicated website (https://land.copernicus.eu/global/hsm, last access: 1 June 2021). This interactive online information system allows access to browse, analyse and download the data, including the accuracy assessment information.

Appendix

A. Satellite data collecting period and type used for LC and LCC mapping

*S-2: Sentinel 2; LS7: Landsat 7; LS8: Landsat 8; SP4: SPOT 4; SP5: SPOT 5; SP6: SPOT 6.

B. Thematic class accuracies per KLC

Accuracy parameters are in per cent; classes with less than 15 samples were not included in the overall accuracy calculation. Accuracy results are presented at the aggregated as well as at the modular LCCS levels, depending on the type of mapping (land cover map – modular; land cover change map – aggregated).

Class: corresponding class (see Table 2 ‘Modular’ or ‘Aggregated’ map code)

PA: producer's accuracy

UA: user's accuracy

NoRP: number of reference points

Author contributions

ZSZ, ABB and AL designed the work and wrote the paper.

Competing interests

The authors declare that they have no conflict of interest.

Disclaimer

All features and data are provided ‘as is’ with no warranties of any kind.

Acknowledgements

Development of the thematic maps was made possible thanks to the efforts of eGEOS (an Italian Space Agency / Telespazio company), ITHACA (Information Technology for Humanitarian Assistance, Cooperation and Action) and Telespazio (a Leonardo / Thales company). The quality evaluations were made possible by IGN FI (France), Joanneum Research (Austria), EOXPLORE (Germany), GISBOX (Romania), Space4environment (Luxembourg), ONFI (France) and LuxSpace (Luxembourg). This work was produced under the European Commission Copernicus Programme, Global Land Service, High Resolution Hot Spot Monitoring component.

Review statement

This paper was edited by David Carlson and reviewed by Nitesh Poona and one anonymous referee.

References

Brink, A., Eva, H., and Bodart, C.: Is Africa Losing Its Natural Vegetation? Monitoring Trajectories of Land-Cover Change Using Landsat Imagery, in: Remote Sensing of Land Use and Land Cover, Principles and Applications, vol. 20120991, edited by: Giri, C., CRC Press, Boca Raton, Florida, 369–376, https://doi.org/10.1201/b11964-28, 2012.

Brink, A. B. and Eva, H. D.: Monitoring 25 years of land cover change dynamics in Africa: A sample based remote sensing approach, 29, 501–512, https://doi.org/10.1016/j.apgeog.2008.10.004, 2009.

Bühne, H. S. to, Wegmann, M., Durant, S. M., Ransom, C., Ornellas, P. de, Grange, S., Beatty, H., and Pettorelli, N.: Protection status and national socio-economic context shape land conversion in and around a key transboundary protected area complex in West Africa, 3, https://doi.org/10.1002/rse2.47, 2017.

Di Gregorio, A.: Land cover classification system: classification concepts and user manual: LCCS, Software version 2., Food and Agriculture Organization of the United Nations, Rome, 190 pp., 2005.
Di Minin, E., Slotow, R., Hunter, L. T. B., Montesino Pouzols, F., Toivonen, T., Verburg, P. H., Leader-Williams, N., Petracca, L., and Moilanen, A.: Global priorities for national carnivore conservation under land use change, 6, https://doi.org/10/f8gmf9, 2016.
European Commission: Science for the AU-EU Partnership building knowledge for sustainable development., Joint Research Centre., 2018.
Foody, G. M.: Valuing map validation: The need for rigorous land cover map accuracy assessment in economic valuations of ecosystem services, 111, 23–28, https://doi.org/10/f65c39, 2015.
Fritz, S., See, L., Perger, C., McCallum, I., Schill, C., Schepaschenko, D., Duerauer, M., Karner, M., Dresel, C., Laso-Bayas, J.-C., Lesiv, M., Moorthy, I., Salk, C. F., Danylo, O., Sturn, T., Albrecht, F., You, L., Kraxner, F., and Obersteiner, M.: A global dataset of crowdsourced land cover and land use reference data, Sci Data, 4, 1–8, https://doi.org/10/gfvcf6, 2017.
Gallaun, H., Steinegger, M., Wack, R., Schardt, M., Kornberger, B., and Schmitt, U.: Remote Sensing Based Two-Stage Sampling for Accuracy Assessment and Area Estimation of Land Cover Changes, Remote Sensing, 7, 11992–12008, https://doi.org/10/f7wzkb, 2015.
Geist, H. J. and Lambin, E. F.: Proximate Causes and Underlying Driving Forces of Tropical Deforestation, BioScience, 52, 143, https://doi.org/10/bmx625, 2002.
Grafius, D. R., Corstanje, R., Warren, P. H., Evans, K. L., Hancock, S., and Harris, J. A.: The impact of land use/land cover scale on modelling urban ecosystem services, Landscape Ecol, 31, 1509–1522, https://doi.org/10.1007/s10980-015-0337-7, 2016.
Güneralp, B., Lwasa, S., Masundire, H., Parnell, S., and Seto, K. C.: Urbanization in Africa: challenges and opportunities for conservation, Environ. Res. Lett., 13, 015002, https://doi.org/10/ggjdfm, 2017.
Haifeng, H., Jianrong, K., Xiaoke, Z., and Kaiyuan, D.: Atmospheric correction of SPOT satellite images based on radiation transfer model, International Conference on Computer Application and System Modeling (ICCASM 2010), https://doi.org/10.1109/ICCASM.2010.5619149, 2010.
Hugo, G.: Patterns and Trends of Urbanization and Urban Growth in Asia, in: Internal Migration, Urbanization and Poverty in Asia: Dynamics and Interrelationships, edited by: Jayanthakumaran, K., Verma, R., Wan, G., and Wilson, E., Springer, Singapore, 13–45, https://doi.org/10.1007/978-981-13-1537-4_2, 2019.
Ide, T., Palmer, L. R., and Barnett, J.: Environmental peacebuilding from below: customary approaches in Timor-Leste, International Affairs, 97, 103–117, https://doi.org/10/ght9rt, 2021.
Kebede, E., Kagochi, J., and Jolly, C. M.: Energy consumption and economic development in Sub-Sahara Africa, Energy Economics, 32, 532–537, https://doi.org/10/fk4cn3, 2010.
Lambin, E. F. and Meyfroidt, P.: Inaugural Article: Global land use change, economic globalization, and the looming land scarcity, 108, 3465–3472, https://doi.org/10/cxqb7q, 2011.
Lang, M. and Tychon, B.: Copernicus Global Land Component Product and Service Detailed Technical Requirements Appendix 1 of Technical Annex, https://land.copernicus.eu/global/documents/applicable, 2015.
Lu, D., Mausel, P., Brondizio, E., and Moran, E.: Change detection techniques, 25, 2365–2401, https://doi.org/10/cx33c5, 2004.
MacKinnon, J., Aveling, C., Olivier, R., Murray, M., Paolini, C., European Commission, and Directorate-General for International Cooperation and Development: Larger than elephants: inputs for an EU strategic approach to wildlife conservation in Africa : synthesis., 2015.
Marshall, M., Norton-Griffiths, M., Herr, H., Lamprey, R., Sheffield, J., Vagen, T., and Okotto-Okotto, J.: Continuous and consistent land use/cover change estimates using socio-ecological data, Earth Syst. Dynam., 8, 55–73, https://doi.org/10/f9s9mg, 2017.
Masek, J. G., Vermote, E. F., Saleous, N. E., Wolfe, R., Hall, F. G., Huemmrich, K. F., Gao, F., Kutler, J., and Lim, T.-K.: A Landsat Surface Reflectance Dataset for North America, 1990–2000, 3, 68–72, https://doi.org/10/b2w5mc, 2006.
van der Meer, E.: Carnivore conservation under land use change: the status of Zimbabwe's cheetah population after land reform, 27, 647–663, https://doi.org/10.1007/s10531-017-1455-0, 2018.

Mora, B., Tsendbazar, N.-E., Herold, M., and Arino, O.: Global Land Cover Mapping: Current Status and Future Trends, in: Land Use and Land Cover Mapping in Europe, vol. 18, edited by: Manakos, I. and Braun, M., Springer Netherlands, Dordrecht, 11–30, https://doi.org/10.1007/978-94-007-7969-3_2, 2014.

Nathaniel, S. P., Nwulu, N., and Bekun, F.: Natural resource, globalization, urbanization, human capital, and environmental degradation in Latin American and Caribbean countries, Environ Sci Pollut Res, 28, 6207–6221, https://doi.org/10/gjfq3b, 2021.

Nissan, H., Goddard, L., de Perez, E. C., Furlow, J., Baethgen, W., Thomson, M. C., and Mason, S. J.: On the use and misuse of climate change projections in international development, WIREs Clim Change, 10, e579, https://doi.org/10/ggfm63, 2019.

Richter, R., Louis, J., and Müller-Wilm, U.: Sentinel-2 msi–level 2a products algorithm theoretical basis document, 1–72, 2012.

Saah, D., Tenneson, K., Poortinga, A., Nguyen, Q., Chishtie, F., Aung, K. S., Markert, K. N., Clinton, N., Anderson, E. R., Cutter, P., Goldstein, J., Housman, I. W., Bhandari, B., Potapov, P. V., Matin, M., Uddin, K., Pham, H. N., Khanal, N., Maharjan, S., Ellenberg, W. L., Bajracharya, B., Bhargava, R., Maus, P., Patterson, M., Flores-Anderson, A. I., Silverman, J., Sovann, C., Do, P. M., Nguyen, G. V., Bounthabandit, S., Aryal, R. R., Myat, S. M., Sato, K., Lindquist, E., Kono, M., Broadhead, J., Towashiraporn, P., and Ganz, D.: Primitives as building blocks for constructing land cover maps, International Journal of Applied Earth Observation and Geoinformation, 85, 101979, https://doi.org/10/ggfq5n, 2020.

Stehman, S. V.: Impact of sample size allocation when using stratified random sampling to estimate accuracy and area of land-cover change, Remote Sensing Letters, 3, 111–120, https://doi.org/10/cfm45t, 2012.

Strobl, P., Baumann, P., Lewis, A., Szantoi, Z., Killough, B., Purss, M. B. J., Craglia, M., Nativi, S., Held, A., and Dhu, T.: The six faces of the data cube, in: Proc. of the 2017 conference on Big Data from Space (BiDS'17), Big Data from Space (BiDS'17), Toulouse, France, 32–35, https://doi.org/10.2760/383579, 2017.

Sylla, M. B., Pal, J. S., Wang, G. L., and Lawrence, P. J.: Impact of land cover characterization on regional climate modeling over West Africa, Clim Dyn, 46, 637–650, https://doi.org/10/f795rb, 2016.

Szantoi, Z., Escobedo, F., Abd-Elrahman, A., Smith, S., and Pearlstine, L.: Analyzing fine-scale wetland composition using high resolution imagery and texture features, 23, 204–212, https://doi.org/10/gdnfvd, 2013.

Szantoi, Z., Brink, A., Buchanan, G., Bastin, L., Lupi, A., Simonetti, D., Mayaux, P., Peedell, S., and Davy, J.: A simple remote sensing based information system for monitoring sites of conservation importance, Remote Sens Ecol Conserv, 2, 16–24, https://doi.org/10.1002/rse2.14, 2016.

Szantoi, Z., Geller, G. N., Tsendbazar, N.-E., See, L., Griffiths, P., Fritz, S., Gong, P., Herold, M., Mora, B., and Obregón, A.: Addressing the need for improved land cover map products for policy support, Environmental Science & Policy, 112, 28–35, https://doi.org/10.1016/j.envsci.2020.04.005, 2020a.

Szantoi, Z., Brink, A., Lupi, A., Mammone, C., and Jaffrain, G.: Key landscapes for conservation land cover and change monitoring, thematic and validation datasets for sub-Saharan Africa, Earth Syst. Sci. Data, 12, 3001–3019, https://doi.org/10.5194/essd-12-3001-2020, 2020b.

Szantoi, Z., Brink, A., and Lupi, A.: Land cover and change thematic and validation datasets for selected African, Caribbean and Pacific areas [Data set], https://doi.org/10.5281/ZENODO.4621375, 2021b.

Szantoi, Z., Brink, A., and Lupi, A.: Land cover and change thematic and validation datasets for selected African, Caribbean and Pacific areas, https://doi.pangaea.de/10.1594/PANGAEA.931968, 2021a

Tewkesbury, A. P., Comber, A. J., Tate, N. J., Lamb, A., and Fisher, P. F.: A critical synthesis of remotely sensed optical image change detection techniques, 160, 1–14, https://doi.org/10/f655gz, 2015.

Tolessa, T., Senbeta, F., and Kidane, M.: The impact of land use/land cover change on ecosystem services in the central highlands of Ethiopia, Ecosystem Services, 23, 47–54, https://doi.org/10/gd54r6, 2017.

Tsendbazar, N.-E., Herold, M., de Bruin, S., Lesiv, M., Fritz, S., Van De Kerchove, R., Buchhorn, M., Duerauer, M., Szantoi, Z., and Pekel, J.-F.: Developing and applying a multi-purpose land cover validation dataset for Africa, Remote Sensing of Environment, 219, 298–309, https://doi.org/10.1016/j.rse.2018.10.025, 2018.

UNEP-WCMC and IUCN: Protected Planet: The World Database on Protected Areas (WDPA) and World Database on Other Effective Area-based Conservation Measures (WD-OECM), https://www.protectedplanet.net/en, March 2021.

Vondou, D. A. and Haensler, A.: Evaluation of simulations with the regional climate model REMO over Central Africa and the effect of increased spatial resolution: EVALUATION OF REMO RESOLUTION OVER CENTRAL AFRICA, Int. J. Climatol, 37, 741–760, https://doi.org/10/gcpxmp, 2017.

Table 1 Mapped key landscapes for conservation within Phase 2.

KLC	Code	Ecoregion (Dinerstein et al., 2017)	Country	Area (km^2)
Updated areas				
Greater Virunga	CAF02	Albertine Rift montane forests Victoria Basin forest-savanna	DRC, Uganda, Rwanda	39 062
Salonga	CAF07	Central Congolian lowland forests	DRC	66 625
Upemba	CAF11	Central Zambezian wet miombo woodlands	DRC	47 318
Yangambi	CAF99	Northeast Congolian lowland forests	DRC	7 276
New areas				
Garamba	CAF05	East Sudanian savanna, Northern Congolian forest-savanna mosaic, Northeastern Congolian lowland forests	DRC, CAR, South Sudan	265 976
Caribbean	CAR01	Windward Islands moist forests, Bahamian-Antillean mangroves, Caribbean shrublands, Lesser Antillean dry forests, Hispaniolan moist forests, Enriquillo wetlands, Hispaniolan dry forests, Hispaniolan pine forests, Bahamian pineyards	AB, Bahamas, Dominica, DR, Haiti, SKN	89 883
Niassa Selous	EAF04	Zambezian flooded grasslands, Eastern Miombo woodlands, Eastern Arc forests, Northern Zanzibar-Inhambane coastal forest mosaic	Tanzania, Mozambique	139 163
Timor-Leste	PAC01	Timor and Wetar deciduous forests	Timor-Leste	14 931
Madagascar	SAF21	Madagascar lowland forests, Madagascar subhumid forests	Madagascar	124 012
Wapok	WAF04	West Sudanian savanna	Ghana, Togo, Benin, Burkina Faso, Niger	57 776

AB: Antigua and Barbuda; CAR: Central African Republic; DR: Dominican Republic; DRC: Democratic Republic of the Congo; SKN: Saint Kitts and Nevis.

Table 2 Dichotomous and Modular thematic land cover/use classes (MCD: mapcode dichotomous level, MCM: mapcode modular level, AG: aggregated classes for land cover change accuracy estimation; see section 3.5 for additional information).

Dichotomous level	MCD	Modular level	MCM	AG
Cultivated and Managed Terrestrial Area (A11)	3	continuous large to medium sized field (>2 ha) of tree crop cover: plantation	31	3
		continuous small sized field (<2 ha) of tree crop cover: plantation	32	3
		continuous large to medium sized field (>2 ha) of tree crop cover: orchard	33	3
		continuous small sized field (<2 ha) of tree crop cover: orchard	34	3
		continuous large to medium sized field (>2 ha) of shrub crop	55	3
		continuous small sized field (<2 ha) of shrub crop	56	3
		continuous large to medium sized field (>2 ha) of herbaceous crop	59	3
		continuous small sized field (<2 ha) of herbaceous crop	60	3
Natural and Semi-Natural Primarily Terrestrial Vegetation (A12)	4	continuous closed (>70-60) trees	77	77
		continuous open general (70-60)-(20-10)% trees	78	78
		continuous closed to open (100-40)% shrubs	112	4
		continuous open (40 - (20-10)%) shrubs	116	4
		continuous closed to open (100-40)% herbaceous vegetation	148	4
		continuous open (40 - (20-10)%) herbaceous vegetation	152	4
Cultivated Aquatic or Regularly Flooded Area (A23)	6	continuous large to medium sized field (>2 ha) of woody crops	155	6
		continuous small sized field (<2 ha) of woody crops	156	6
		continuous large to medium sized field (>2 ha) of graminoid crops	159	6
		continuous small sized field (<2 ha) of graminoid crops	160	6
Natural And Semi-Natural Aquatic or Regularly Flooded Vegetation (A24)	7	closed (>70-60)% trees	165	165
		open general (70-60)-(20-10)% trees	166	165
		closed to open (100-40)% shrubs	171	7
		very open (40 - (20-10)%) shrubs	175	7

		closed to open (100-40)% herbaceous vegetation	178	7
		very open (40 - (20-10)%) herbaceous vegetation	182	7
Artificial Surfaces and Associated Area (B15)	10	built up area	184	184
		non built up area	185	185
Bare Area (B16)	11	Bare area	11	11
Artificial Waterbodies, Snow and Ice (B27)	13	artificial waterbodies (flowing)	186	13
		artificial waterbodies (standing)	187	13
Natural Waterbodies, Snow and Ice (B28)	14	natural waterbodies (flowing)	190	14
		natural waterbodies (standing)	191	14
		snow	192	14
		ice	193	14
Not Inland Cover	99	not terrestrial cover	999	999

525

Table 3 Validation dataset attributes

KLC Code	Land cover		Land cover change		Number of points
	Number of classes	Mapping year	Number of classes	Mapping year	
Updated areas					
CAF02	27	2015	21	2019	2998
CAF07	17	2016	16	2019	3069
CAF11	23	2016	19	2019	3228
CAF99	17	2016	20	2019	2421
New areas					
CAF05	24	2017	17	2019	4647
			17	2000	7168
CAR01	29	2017	26	2000	4029
EAF04	26	2017	18	2000	3943
PAC01	28	2016	26 30 28	2000 2005 2010	4413
SAF21	29	2017	18	2000	3995
WAF04	24	2017	18	2000	3522

Table 4 Overall accuracies achieved for land cover mapping (%).

	LC map	Reference date	LCC map	Reference date
Updated thematic maps				
CAF02	90.09	2015	99.38	2019
CAF02	90.09	2015	91.93	2001
CAF07	98.38	2016	98.36	2019
CAF11	95.27	2016	95.81	2019
CAF11	95.87	2016	95.81	2019
CAF99	98.51	2016	99.31	2019
CAF99	99.21	2016	99.31	2019
New thematic maps				
CAF05	90.63	2015	91.63	2019
	91.75	2015	92.35	2000
CAR01	92.55	2017	93.41	2000
EAF04	97.30	2017	97.80	2000
PAC01	91.28	2016	93.55	2000
			93.26	2005
			94.24	2010
SAF21	91.00	2017	92.30	2000
WAF04	97.20	2015	97.50	2000

LC - land cover, LCC - land cover change

Figure 1 Spatial distribution of the key landscapes for conservation Phase 2 areas.

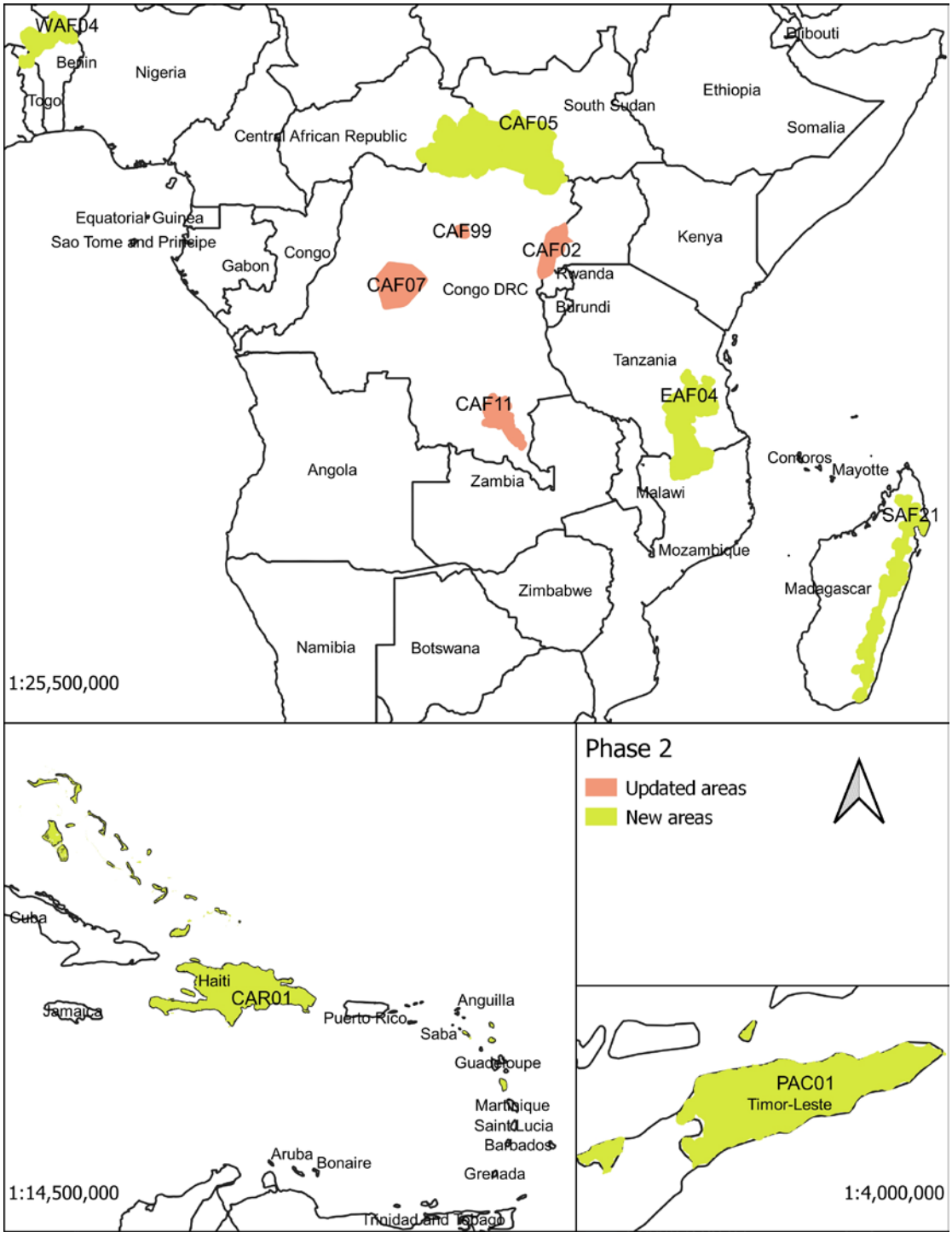

Figure 2 Overall production workflow

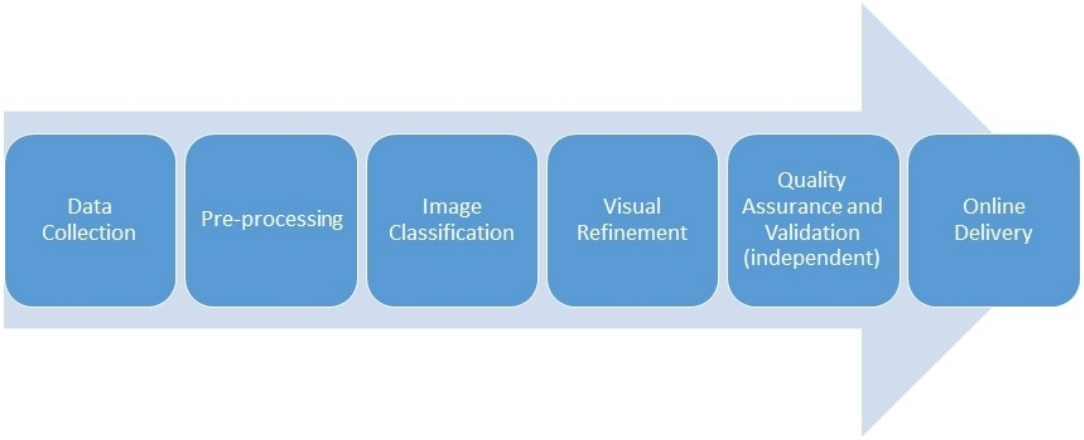

Figure 3 Spatial distribution of the validation datasets within the updated key landscapes for conservation.

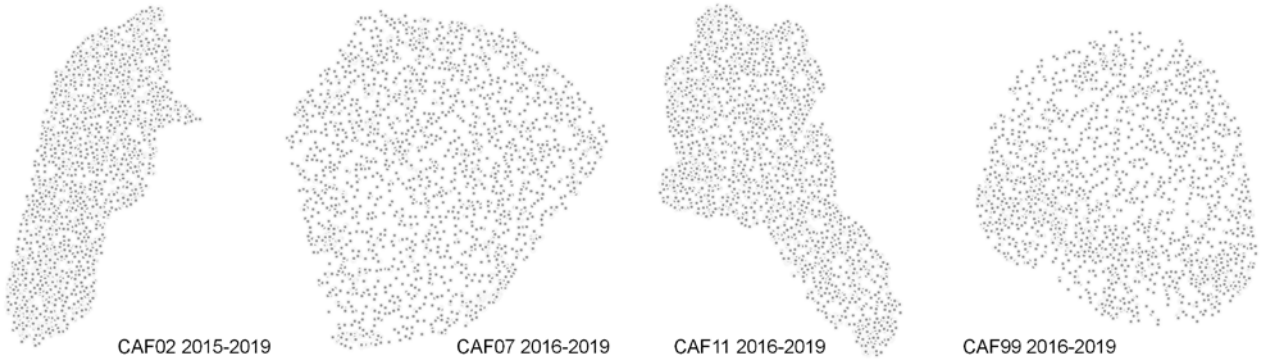

Figure 4 Spatial distribution of the validation datasets within the new key landscapes for conservation.

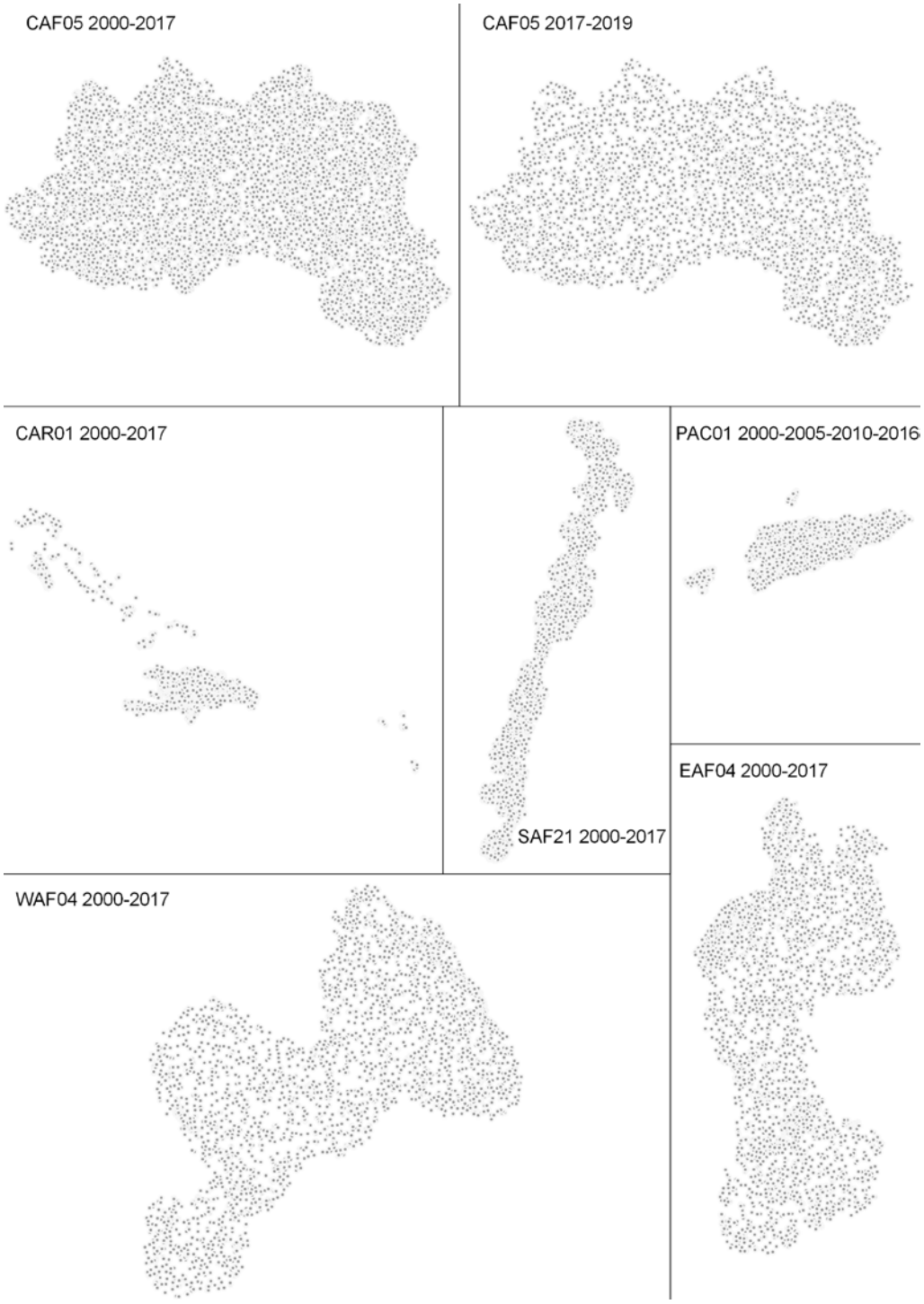

545

Figure 5 Key Landscapes for Conservation - modular classification level. The boundaries (black polygons) represent protected areas (IUCN category I-IV – UNEP-WCMC and IUCN, 2021) within the KLCs. Both land cover and land cover change maps are presented for each KLC.

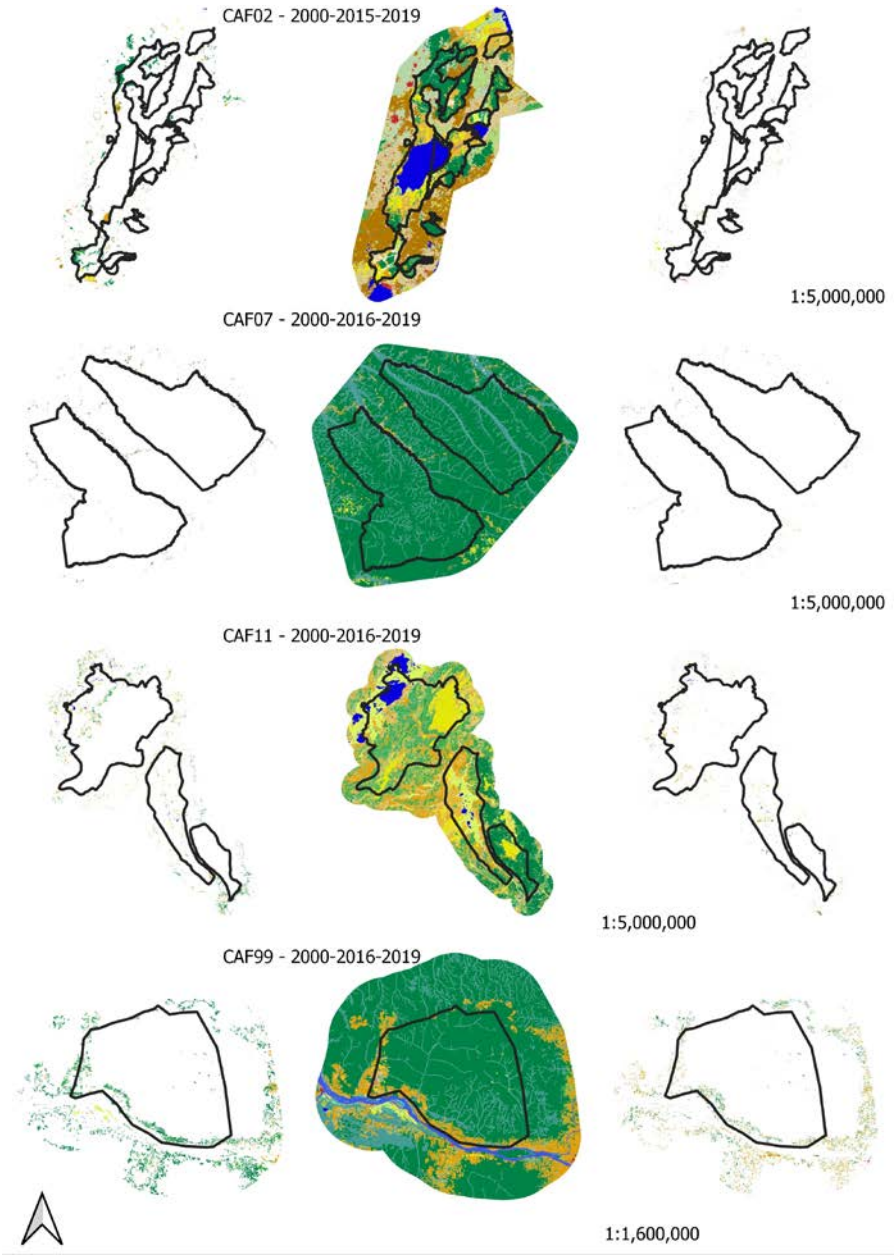

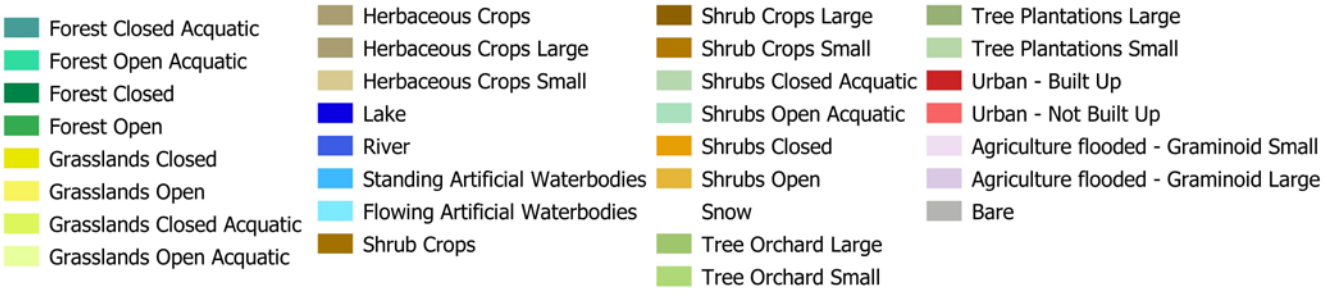

*CAF02: Greater Virunga; CAF07: Salonga; CAF11: Upemba; CAF99: Yangambi. Year 2000 datasets are available in Szantoi et al. (2020b).

555

Figure 6 Key landscapes for conservation - modular classification level. The boundaries (black polygons) represent protected areas (IUCN category I-IV – UNEP-WCMC and IUCN, 2021) within the KLCs. Both land cover and land cover change maps are presented for each KLC. The inlets show the south-east part of the Caribbean KLC.

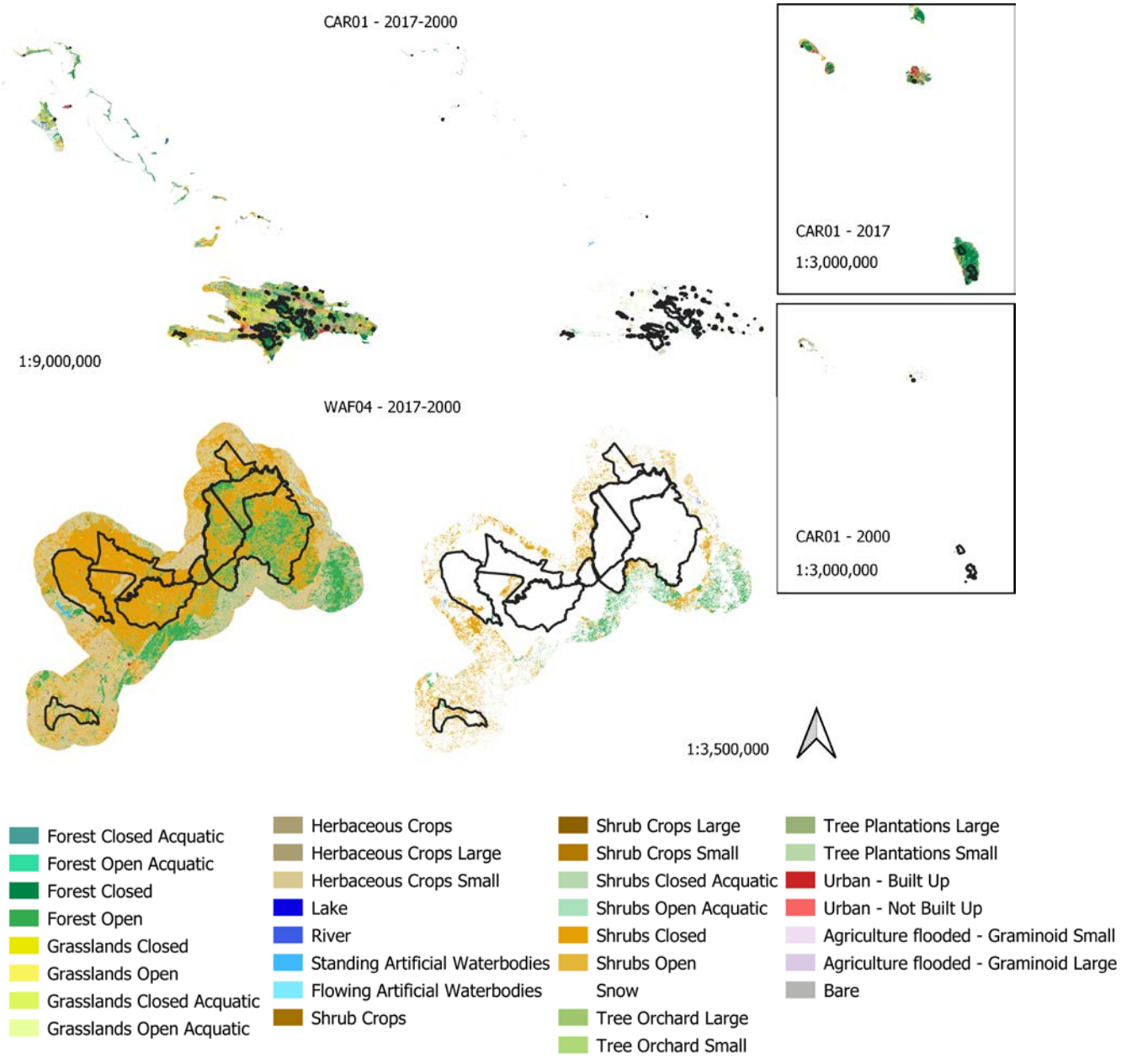

560

*CAR01: Caribbean; WAF04: Wapok.

Figure 7 Key Landscapes for Conservation - modular classification level. The boundaries (black polygons) represent protected areas (IUCN category I-IV – UNEP-WCMC and IUCN, 2021) within the KLCs. Both land cover and land cover change maps are presented for each KLC.

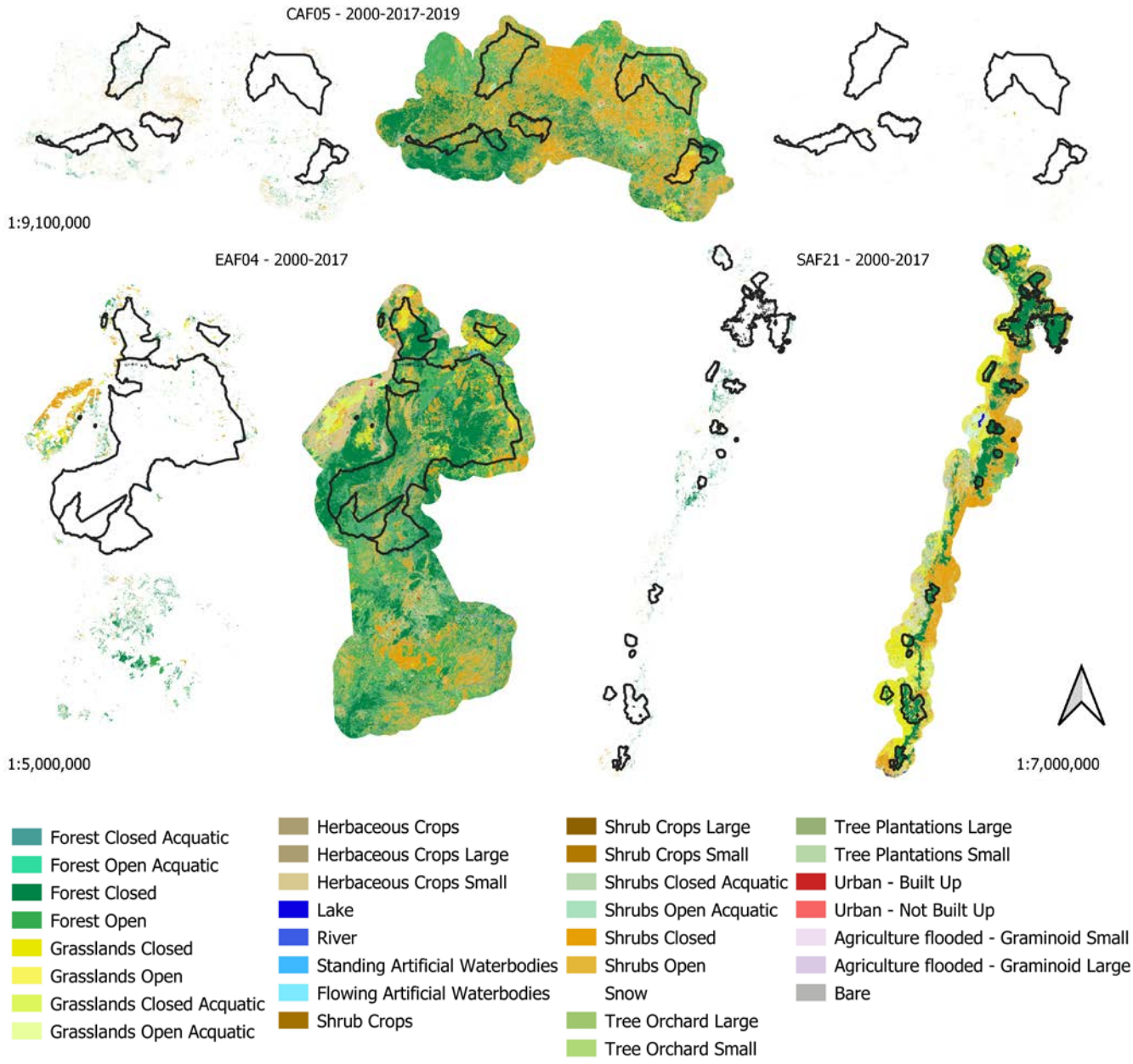

*CAF05: Garamba; EAF04: Niassa Selous; SAF21: Madagascar.

Figure 8 Timor-Leste Key Landscape for Conservation - modular classification level. The boundaries (black polygons) represent the country boundary. Both land cover and land cover change maps are presented for Timor-Leste.

575

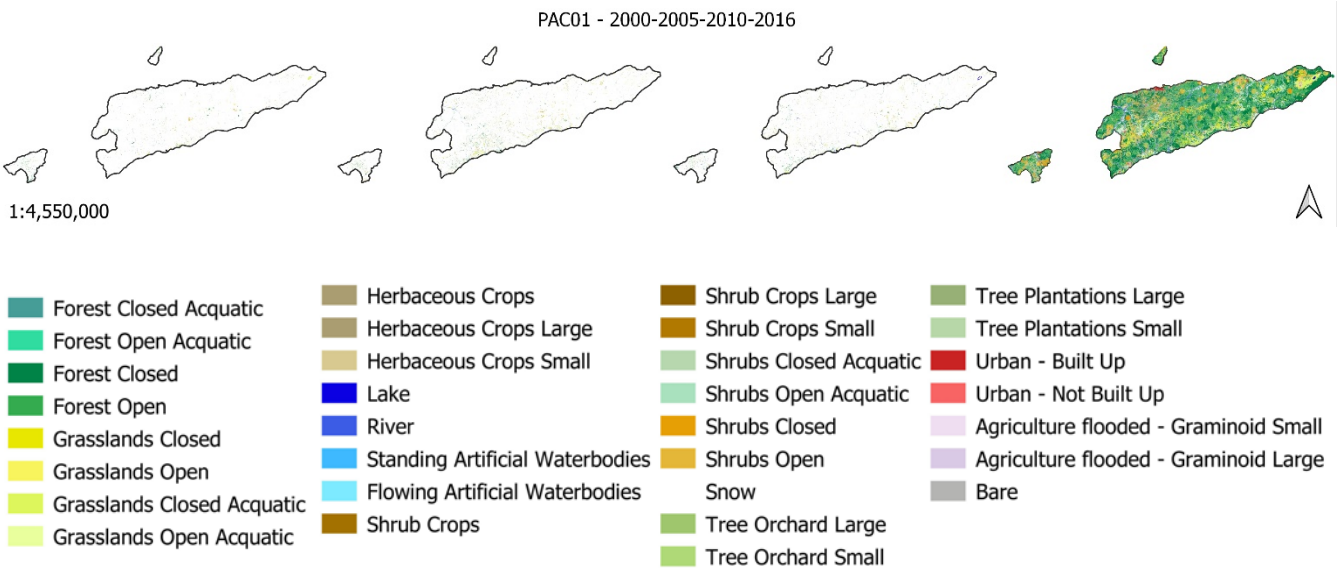

Appendix

A. Satellite data collecting period and type used for LC and LCC mapping

KLC	LC map	Data period	Data type*	LCC map	Data period	Data type*
CAF02	2015	07/2013 - 10/2016	LS8	2019	01/2019 - 12/2019	S-2
CAF07	2016	05/2013 - 10/2016	LS8	2019	01/2019 - 01/2020	S-2
CAF11	2016	01/2015 - 06/2016	LS8	2019	01/2019 - 10/2019	S-2
CAF99	2016	03/2014 - 11/2016	LS8	2019	02/2019 - 12/2019	S-2
CAF05	2017	12/2014 - 01/2018	LS8	2019 2000	02/2019 - 11/2019 11/1999 - 01/2003	S-2 LS7
CAR01	2017	05/2016 - 12/2017	S-2	2000	02/1999 - 11/2004	SP4, LS7
EAF04	2017	04/2016 - 10/2017	S-2	2000	07/1999 - 06/2002	LS7
PAC01	2016	12/2015 - 11/2016	S-2	2000 2005 2010	04/2001 - 11/2002 04/2003 - 12/2007 01/2008 - 10/2012	SP4, SP5 SP5 SP5, SP6
SAF21	2017	06/2016 - 11/2017	S-2	2000	10/1999 - 12/2002	LS7
WAF04	2017	11/2016 - 03/2018	S-2	2000	09/1998 - 06/2003	SP4, SP5

*S-2: Sentinel 2; LS7: Landsat 7; LS8: Landsat 8; SPOT 4: SP4; SPOT 5: SP5; SPOT 6: SP6.

B. Thematic class accuracies per KLC.

Accuracy parameters are in percent, classes with less than 15 samples were not included in the overall accuracy calculation. Accuracy results are presented at the aggregated as well as at the modular LCCS levels, depending on the type of mapping (land cover map - modular, or land cover change map - aggregated).

Class: corresponding class (see Table 2 “Modular” or “Aggregated” map code)

PA: producer's accuracy

UA: user's accuracy

NoRP: number of reference points

CAF02 (aggregated)						
	2015			2019		
Class	PA	UA	NoRP	PA	UA	NoRP
3	99.7	99.7	1277	99.7	99.6	1243

4	98.8	97.7	510	98.8	98.2	541
6	0	0	0	0	0	0
7	100	99	120	100	99	148
11	96.8	93.4	28	100	93.3	20
14	100	100	219	100	100	175
77	100	99.9	648	99.9	100	508
78	92.6	100	133	92.3	98.4	217
165	100	100	3	100	100	2
166	100	100	5	100	100	2
184	99.9	100	52	100	99.9	129
185	100	100	2	100	100	10

595

CAF05 (aggregated)									
	2000			2015			2019		
Class	PA	UA	NoRP	PA	UA	NoRP	PA	UA	NoRP
3	92.8	76.9	396	85	92.4	249	85.9	89.6	211
4	91.4	95	2957	93.5	91.4	1720	93.4	91.3	1764
7	98.7	84.2	317	82.5	87.3	150	82.5	87.3	149
11	98.3	93.5	59	83.8	100	10	83.8	100	10
13	100	100	8	100	100	14	100	100	15
14	95.4	93.9	96	99.9	100	22	99.9	100	21
77	94.1	96.4	1956	94.8	96.2	1399	94.6	96.2	1283
78	90.7	83	1205	85.7	86.2	917	85.6	86.2	949
165	0	0	0	0	0	1	0	0	1
166	100	83.7	41	100	100	1	100	100	1
184	96.8	94.3	88	82.7	97.6	92	81.6	97.4	155
185	100	23.1	9	100	93.2	70	94.9	94	87

CAF05 (all classes – LC map)			
2015			
Class	PA	UA	NoRP
11	98.3	93.5	59
31	100	99.9	127
32	5.9	92.3	14
34	100	100	1
56	90	92.4	67
59	0	0	0

60	85.1	83	209
77	95.1	95.8	1954
78	89.9	82.8	1184
112	88.8	93.2	2355
116	81.2	74.9	285
148	72.6	84.2	215
152	94.4	93.6	9
165	0	0	0
166	100	85.1	40
171	98.4	73.7	82
175	98.8	95.6	75
178	98.1	87.2	152
182	87.5	28	8
184	95.1	95.8	161
185	100	100	50
187	100	100	8
190	95.4	94	80
191	100	95.8	23

600

CAF07 (all classes – LC/LCC map)							
2016				2019			
Class	PA	UA	NoRP	Class	PA	UA	NoRP
11	100	100	2	11	100	100	2
31	96.6	83.6	53	31	95.9	84.2	52
32	96.4	66.7	3	32	97.6	33.3	4
56	95.1	77.5	91	56	87.8	75.8	112
60	91.3	89.8	102	60	91.3	72.6	89
77	98.4	99.8	1605	77	98.5	99.8	1524
78	82.7	92.7	98	78	90.1	94.9	124
112	89.5	86.1	231	112	89	88.6	297
116	96.2	96.8	61	116	82.8	90	30
148	99.8	97.4	134	148	99.4	97.5	144
165	99.3	92.3	386	152	0	0	0
166	31.6	75	19	165	99.3	92.3	379
171	94.1	94.3	54	166	31.6	47.2	19
175	0	0	2	171	94.5	94	65
178	100	85	51	175	50	100	4

184	83.1	90.4	77	178	92.1	85.4	38
190	87.8	93.8	77	184	81	90.5	87
191	100	100	22	190	87.7	92.6	76
				191	100	100	22

CAF11 (aggregated)									
2000				2016			2019		
Class	PA	UA	NoRP	PA	UA	NoRP	PA	UA	NoRP
3	98.7	92.8	339	92.9	95.1	201	93	96.2	272
4	99.3	93.8	1169	99.2	92.4	1099	99.2	92.2	999
6	100	14.4	2	42.4	100	33	42.5	100	33
7	96.9	99.2	614	97.8	96.5	373	97.9	96.8	372
11	100	96.7	30	0	0	0	0	0	0
14	98.7	99.9	275	99.8	99.4	120	100	99.8	111
77	94.5	95.6	529	90.5	98.9	515	90.4	98.8	430
78	92.6	97.7	597	95	98.4	711	94.8	98.3	760
165	79.4	96.3	79	77.1	100	7	77	100	5
166	98.7	99.2	47	99.8	99.3	12	99.8	99.2	11
184	100	95.8	87	99.9	94.6	81	100	94.9	157
185	100	95.4	17	100	100	76	93.8	100	78

CAF11 (all classes – LC map)			
2015			
Class	PA	UA	NoRP
11	100	100	30
32	100	100	26
34	0	0	0
56	69.9	100	1
59	92.4	99.1	74
60	97.3	97.1	339
77	94.6	95.2	488
78	92.4	97.1	534
112	96.8	86.9	441
116	97.7	94.3	289
148	98.5	97.1	325
152	0	0	0
160	100	100	3

165	79.1	96.2	78
166	96.9	99.2	46
171	75	92.7	74
175	56.8	98.6	72
178	97.9	98	411
182	95	95	20
184	100	98.9	167
185	100	100	75
190	87.9	98.2	90
191	99.8	100	202

605

CAF99 (aggregated)									
	2000			2016			2019		
Class	PA	UA	NoRP	PA	UA	NoRP	PA	UA	NoRP
3	91.6	98.9	431	85.9	98	241	86.2	98.7	193
4	92.4	92.1	417	98.4	96.4	397	99.5	97.5	452
7	100	97.8	231	99.8	88	72	94.7	88.8	76
14	100	100	175	100	100	108	100	100	109
77	99	99.2	905	99.7	99.9	1139	99.7	99.9	1098
78	93.6	85.1	210	97	99.8	60	92.1	93.1	43
165	97.8	97.9	246	100	99.1	352	100	99.1	346
166	100	88.7	40	100	82.2	22	99.8	81.6	16
184	99.4	88.3	72	99.4	100	28	98.7	99.8	85
185	0	0	0	0	0	0	0	0	0

CAF99 (all classes – LC map)			
2015			
Class	PA	UA	NoRP
31	91.6	99.8	267
32	94.5	100	69
56	100	99.5	76
59	100	9.5	4
60	91.9	96.5	125
77	99.6	99.2	732
78	79.1	91.5	156
112	96.1	95.9	341
148	98.7	96.9	168

165	97.8	97.5	240
166	100	89.2	42
171	100	100	102
175	0	0	3
178	100	91.6	77
184	100	95.9	150
185	100	100	2
190	100	100	113
191	100	100	60

610

CAR01							
Aggregated classes				All classes – LC map			
2000				2017			
Class	PA	UA	NoRP	Class	PA	UA	NoRP
3	90.8	94.5	874	11	91.9	86.5	79
4	90.1	96.1	890	31	83.1	83.2	110
6	98.8	97.3	160	32	98.9	84.5	65
7	93	92.1	343	33	80.6	79.8	65
11	83.7	82.7	70	34	100	81.9	24
13	99.8	83.5	155	55	98.3	86.2	71
14	89.7	93.6	181	56	100	92.9	87
77	97.9	90.6	519	59	91	92.3	159
78	92.5	88.6	346	60	85.8	92.2	272
165	96	89.7	61	77	97.8	93.3	513
166	100	92.3	57	78	89.4	88.5	332
184	92.5	98.1	122	112	90.4	93.4	379
185	100	97.2	64	116	92.3	94.6	116
999	99.6	98.2	173	148	88.5	89.5	270
				152	100	92.8	63
				159	96	97.5	81
				160	82.1	97.5	85
				165	94.8	89.6	63
				166	100	91.8	56
				171	90.7	90.9	102
				175	93.4	95.3	85
				178	95.5	84.6	92
				182	98.9	82.6	58

				184	92.2	99.8	209
				185	100	97	75
				186	96.2	93.3	71
				187	97.6	87.5	81
				190	97.5	92.7	79
				191	87	100	112
				999	99.7	98.2	172

EAF04							
Aggregated classes				All classes – LC map			
2000				2017			
Class	PA	UA	NoRP	Class	PA	UA	NoRP
3	93.4	95	638	11	100	98.7	86
4	96.8	96.3	834	31	100	79.4	43
6	83	82.1	130	32	100	100	12
7	92.4	95.7	260	33	100	97.6	129
11	100	98.7	86	34	90.9	99.6	97
14	99.5	97.9	172	55	100	99.8	78
77	99.3	98.5	952	56	100	93.8	30
78	97.3	98.5	723	59	100	100	82
165	100	100	51	60	96.8	94.4	269
166	0	0	2	77	98.8	98	922
184	99.6	97.4	90	78	96.6	98.4	652
185	100	83.3	5	112	95.6	95.1	465
				116	91.3	97.8	114
				148	99.7	94.8	135
				152	100	77.3	17
				159	0	0	0
				160	93.7	99.5	138
				165	100	100	51
				166	0	0	2
				171	100	91	35
				175	60.9	83.4	11
				178	92.3	95.1	211
				184	99.8	100	171
				185	100	92	23

				190	99.8	98.9	92
				191	100	98.5	78

615

PAC01 (aggregated classes)											
2000				2005				2010			
Class	PA	UA	NoRP	Class	PA	UA	NoRP	Class	PA	UA	NoRP
3	89.6	89.5	603	3	87.9	89.4	602	3	92.2	91.5	600
4	88.2	96.3	983	4	88	96.2	967	4	92	95.4	908
6	95.9	93.9	158	6	95.7	94.7	147	6	94	93.6	151
7	96.2	96.4	380	7	95.6	96	361	7	93.6	93.9	341
11	81.1	88.2	86	11	97.7	88	81	11	93.5	88.2	87
13	94.1	88.9	34	13	94.2	86.7	35	13	96.4	93	38
14	90.4	93.9	269	14	91	94.8	303	14	91.1	94.8	334
77	98.2	91.8	713	77	98.2	91.2	707	77	97.5	93.5	722
78	92.4	95	821	78	91.8	94.7	805	78	92.3	95.3	811
165	92.6	93.7	88	165	89.8	94.2	87	165	92.9	93	75
166	93.2	99.2	78	166	90.8	98.8	75	166	96.7	98.8	72
184	94.3	91.7	120	184	94.4	93	163	184	95	96	190
185	100	94.9	12	185	100	95.1	13	185	97.3	100	17
999	96.3	78	61	999	96.3	78	61	999	96.3	78	61

PAC01 (all classes – LC map)			
2016			
Class	PA	UA	NoRP
11	96.4	91.1	89
31	87.2	96.8	70
32	94.5	85.2	50
33	0	0	1
34	0	0	1
55	60.8	100	13
56	99.2	96.4	29
60	93.1	88.1	386
91	95.8	90.8	536
92	83.2	87.5	236
95	96.5	89.2	390
96	84.6	95.9	423

123	89.3	78.8	132
124	88.9	97.8	160
139	98.9	87.2	100
140	96.3	89.9	113
148	89.5	94	356
152	0	0	3
160	92.1	94.4	140
165	94.1	90.4	78
166	89	98.7	75
171	98.4	93.4	53
175	98.3	92.9	72
178	95.5	95.3	212
182	100	95.7	14
184	91.7	96.1	234
185	96.3	100	23
187	96	95.3	44
190	88.7	94.3	277
191	100	97.3	29
999	96.3	78	61

620

SAF21							
Aggregated classes				All classes – LC map			
2000				2017			
Class	PA	UA	NoRP	Class	PA	UA	NoRP
3	89.5	84	517	11	95.3	92.8	67
4	94.9	92.4	1352	31	83.8	91.6	110
6	75.2	80.6	269	32	2.5	30.4	14
7	84	82.7	238	33	25	100	12
11	95.3	94.2	68	34	99.7	96.5	69
13	89.2	98	140	55	98.8	97.3	75
14	83.2	96.4	176	56	100	34.1	14
77	93	97.2	856	59	98.3	98.2	59
78	87.8	82.2	228	60	88.3	82.6	179
165	100	11.9	5	77	94.4	96.4	692
166	0.4	16.7	13	78	88	81.8	253
184	100	76.4	81	112	93	88.4	725
185	96	94.1	50	116	94.3	80.7	79

999	0	0	1	148	89.8	93.8	530
				152	84.7	85.4	47
				156	0	0	1
				159	100	14.7	5
				160	76	81.5	273
				165	100	11.9	5
				166	0.4	16.7	13
				171	100	79.1	84
				175	67.6	96.6	19
				178	85.5	83.5	125
				182	12.9	66.7	3
				184	100	94.5	153
				185	99.7	99.4	72
				186	100	94.1	64
				187	87.9	98.6	76
				190	79.7	97.6	99
				191	95.4	93.3	76
				999	0	0	1

625

WAF04							
Aggregated classes				All classes – LC map			
2000				2015			
Class	PA	UA	NoRP	Class	PA	UA	NoRP
3	99.5	93.7	670	11	100	100	48
4	97.4	98.8	1345	31	100	100	9
6	91.7	84.5	67	32	80	100	5
7	98.6	95.3	239	33	92.8	100	17
11	100	100	47	34	99.1	99	75
13	97	100	108	60	99.5	98.1	726
14	97.7	97.3	162	77	97.9	95.2	146
77	95.5	97.4	151	78	97.1	98.3	487
78	96	98.2	537	112	98.3	96.3	756
165	100	73.3	21	116	86.1	98.1	297
166	98.6	93.7	60	148	83.6	98.9	90
184	100	97.5	83	152	98.7	99.5	40
185	100	100	8	160	81.8	89	82
				165	100	72.4	20

				166	98.5	92.5	59
				171	92.7	95	59
				175	96.5	98.6	32
				178	97.3	72.5	142
				182	100	97.5	29
				184	100	97.8	151
				185	100	100	10
				187	100	100	79
				190	97.6	98.7	79
				191	97.7	97.3	70